NUCLEAR MEAN FIELDS PRODUCED FROM SEMI-REALISTIC NUCLEONIC INTERACTION*

H. Nakada

Department of Physics, Graduate School of Science, Chiba University
Yayoi-cho 1-33, Inage, Chiba 263-8522, Japan

(Received November 10, 2015)

Recent applications of the semi-realistic nucleonic interaction to the nuclear mean fields are presented: *(i)* prediction of magic numbers in the whole nuclear chart and *(ii)* isotope shifts of the $Z =$ magic nuclei with the density-dependent LS interaction. In *(i)*, it is found that the known magic numbers are well reproduced with only a few exceptions, from light to heavy stable and unstable nuclei, with the M3Y-P6 interaction. A part of this success is attributed to the realistic tensor force included in the interaction. In *(ii)*, the kink of the Pb nuclei and the vanishing isotope shift of ^{48}Ca relative to ^{40}Ca, both of which have supplied long-standing problems, can be described fairly well, if we take into account the density-dependence in the LS channel indicated by the chiral effective field theory. These results illustrate that a proper combination of microscopic theories and phenomenology on effective interactions can advance nuclear structure physics.

DOI:10.5506/APhysPolBSupp.8.629
PACS numbers: 21.60.Jz, 21.30.Fe, 21.10.Pc, 21.10.Ft

1. Introduction

As being able to describe basic properties of nuclei such as the saturation and the shell structure, importance of the mean-field (MF) or the energy density functional (EDF) approaches in nuclear structure theories cannot be exaggerated. However, origin of the spin-orbit (ℓs) splitting, which is essential to the nuclear shell structure, has not been understood well [1]. Moreover, experiments using the radioactive beams disclosed that the shell structure significantly depends on the proton (Z) and neutron (N) numbers [2], and this Z- and N-dependence was not well predicted by the conventional MF approaches. This suggests that the effective nucleonic interaction (or EDF) should be reconsidered.

* Presented at the XXII Nuclear Physics Workshop "Marie and Pierre Curie", Kazimierz Dolny, Poland, September 22–27, 2015.

I have developed a series of semi-realistic nucleonic interactions [3, 4], which have a root on the bare nucleonic interaction but contain phenomenological modifications, and have used them in the calculations in the MF [5,6] and the random-phase approximations [7, 8]. The semi-realistic interaction used in this study is based on the Michigan three-range Yukawa (M3Y) interaction which was derived from the Paris two-nucleon ($2N$) interaction via the G-matrix [9]. To obtain the saturation properties, density-dependent contact terms are added to the central channels, and some of the strength parameters are modified accordingly. Since it is difficult to account for the observed size of the ℓs splitting, the LS channel of the M3Y interaction has been modified in a phenomenological manner [3], or in a manner inspired by results of the chiral effective field theory (χEFT) [10]. In this paper, I shall show recent results on the shell structure of the MF calculations with the M3Y-type semi-realistic interaction: prediction of the magic numbers in Sec. 3 and investigation on the isotope shifts of the $Z =$ magic nuclei in Sec. 4.

2. Mean-field approaches with semi-realistic interaction

The full Hamiltonians for the MF calculations is given by $H = H_\mathrm{N} + V_\mathrm{C} - H_\mathrm{cm}$, with the Coulomb interaction V_C, the center-of-mass Hamiltonian $H_\mathrm{cm} = \boldsymbol{P}^2/2AM$ and the nuclear part $H_\mathrm{N} = \sum_i \boldsymbol{p}_i^2/2M + \sum_{i<j} \hat{v}_{ij}$. The following form is taken for effective nucleonic interaction $\hat{v}_{ij}$:

$$\begin{aligned}
\hat{v}_{ij} &= \hat{v}_{ij}^{(\mathrm{C})} + \hat{v}_{ij}^{(\mathrm{LS})} + \hat{v}_{ij}^{(\mathrm{TN})} + \hat{v}_{ij}^{(\mathrm{C}\rho)} \left(+\hat{v}_{ij}^{(\mathrm{LS}\rho)}\right) , \\
\hat{v}_{ij}^{(\mathrm{C})} &= \sum_n \left(t_n^{(\mathrm{SE})} P_\mathrm{SE} + t_n^{(\mathrm{TE})} P_\mathrm{TE} + t_n^{(\mathrm{SO})} P_\mathrm{SO} + t_n^{(\mathrm{TO})} P_\mathrm{TO}\right) f_n^{(\mathrm{C})}(r_{ij}) , \\
\hat{v}_{ij}^{(\mathrm{LS})} &= \sum_n \left(t_n^{(\mathrm{LSE})} P_\mathrm{TE} + t_n^{(\mathrm{LSO})} P_\mathrm{TO}\right) f_n^{(\mathrm{LS})}(r_{ij})\, \boldsymbol{L}_{ij} \cdot (\boldsymbol{s}_i + \boldsymbol{s}_j) , \\
\hat{v}_{ij}^{(\mathrm{TN})} &= \sum_n \left(t_n^{(\mathrm{TNE})} P_\mathrm{TE} + t_n^{(\mathrm{TNO})} P_\mathrm{TO}\right) f_n^{(\mathrm{TN})}(r_{ij})\, r_{ij}^2 S_{ij} , \\
\hat{v}_{ij}^{(\mathrm{C}\rho)} &= \left(C^{(\mathrm{SE})}[\rho(\boldsymbol{r}_i)]\, P_\mathrm{SE} + C^{(\mathrm{TE})}[\rho(\boldsymbol{r}_i)]\, P_\mathrm{TE}\right) \delta(\boldsymbol{r}_{ij}) , \\
\hat{v}_{ij}^{(\mathrm{LS}\rho)} &= 2i\, D[\rho(\boldsymbol{R}_{ij})]\, \boldsymbol{p}_{ij} \times \delta(\boldsymbol{r}_{ij})\, \boldsymbol{p}_{ij} \cdot (\boldsymbol{s}_i + \mathbf{s}_j) .
\end{aligned} \tag{1}$$

Here $\boldsymbol{L}_{ij} = \boldsymbol{r}_{ij} \times \boldsymbol{p}_{ij}$, $S_{ij} = 3(\boldsymbol{s}_i \cdot \hat{\boldsymbol{r}}_{ij})(\boldsymbol{s}_j \cdot \hat{\boldsymbol{r}}_{ij}) - \boldsymbol{s}_i \cdot \boldsymbol{s}_j$, and $f_n(r) = e^{-\mu_n r}/\mu_n r$. P_Y represents the projection operator on the channel Y, where Y is a singlet-even (SE), a triplet-even (TE), a singlet-odd (SO) or a triplet-odd (TO) $2N$ channel. For $\hat{v}_{ij}^{(\mathrm{C}\rho)}$, we take $C^{(\mathrm{Y})}[\rho] = t_\rho^{(\mathrm{Y})} \rho^{\alpha^{(\mathrm{Y})}}$ (Y = SE or TE, $\alpha^{(\mathrm{SE})} = 1$, $\alpha^{(\mathrm{TE})} = 1/3$). For $D[\rho]$ in $\hat{v}_{ij}^{(\mathrm{LS}\rho)}$ that is used in Sec. 4, we adopt the form $D[\rho(\boldsymbol{r})] = -w_1\, \rho(\boldsymbol{r})/[1 + d_1 \rho(\boldsymbol{r})]$. To the MF calculations, the numerical algorithm based on the Gaussian expansion method [11–13] is applied.

Some of the parameters in the central channels have been fitted to the experimental data of the binding energies and the matter radii of doubly magic nuclei from ^{16}O to ^{208}Pb [4], whereas $\hat{v}_{ij}^{(\mathrm{TN})}$ and the longest-range part of $\hat{v}_{ij}^{(\mathrm{C})}$ (that comes from the one-pion exchange and is denoted by $\hat{v}_{\mathrm{OPEP}}^{(\mathrm{C})}$) are realistic, being unchanged from the M3Y-Paris interaction. Results with the parameter-set M3Y-P6 and its variant will be shown in this paper. In M3Y-P6, $\hat{v}_{ij}^{(\mathrm{LS})}$ is enhanced by an overall factor 2.2, to reproduce the single-particle (s.p.) level sequence at ^{208}Pb [4].

It has been pointed out that the tensor channels in the $2N$ interaction play important roles in the Z- or N-dependence of the shell structure [14]. Since the semi-realistic interactions contain the realistic tensor force, it will be interesting to check how well it describes the Z- or N-dependence of the shell structure. Although the s.p. energies obtained by the MF calculations do not correspond to the observed levels, which are affected by the coupling to *e.g.* the vibrational degrees of freedom, the energies calculated in the MF regime can be compared with the energies averaged by the spectroscopic factors. A good example is found in the $p0d_{3/2}^{-1}$ and $p1s_{1/2}^{-1}$ states of ^{40}Ca and ^{48}Ca, for which the sum of the observed spectroscopic factors is close to unity [15,16]. Moreover, these two states are inverted from ^{40}Ca to ^{48}Ca. In Fig. 1, the s.p. energy difference between $p0d_{3/2}$ and $p1s_{1/2}$ in the spherical Hartree–Fock (HF) calculations is compared with the data averaged by the spectroscopic factors. As well as the inversion from ^{40}Ca to ^{48}Ca, the slope of the s.p. energy difference is well reproduced by the semi-realistic interaction M3Y-P6. It is also found that this slope is hard to be reproduced with *e.g.* the Gogny interaction D1M, which do not have the tensor channels. Effects of $\hat{v}_{ij}^{(\mathrm{TN})}$ on the slope are argued in detail in Ref. [17].

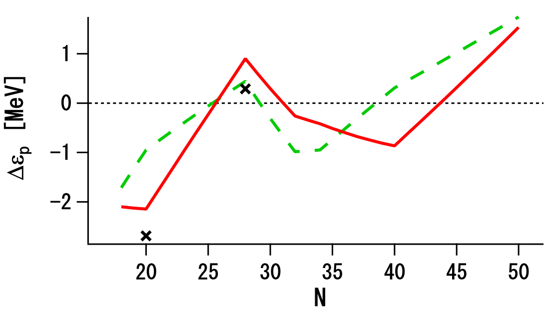

Fig. 1. (Color on-line) $\Delta\varepsilon_p = \varepsilon_p(1s_{1/2}) - \varepsilon_p(0d_{3/2})$ in Ca. Solid (red) and dashed (green) line is obtained by the HF calculation with M3Y-P6 and D1M, respectively. Experimental data for ^{40}Ca and ^{48}Ca are shown by crosses, obtained from the spectroscopic factors given in Refs. [15,16].

3. Magic numbers

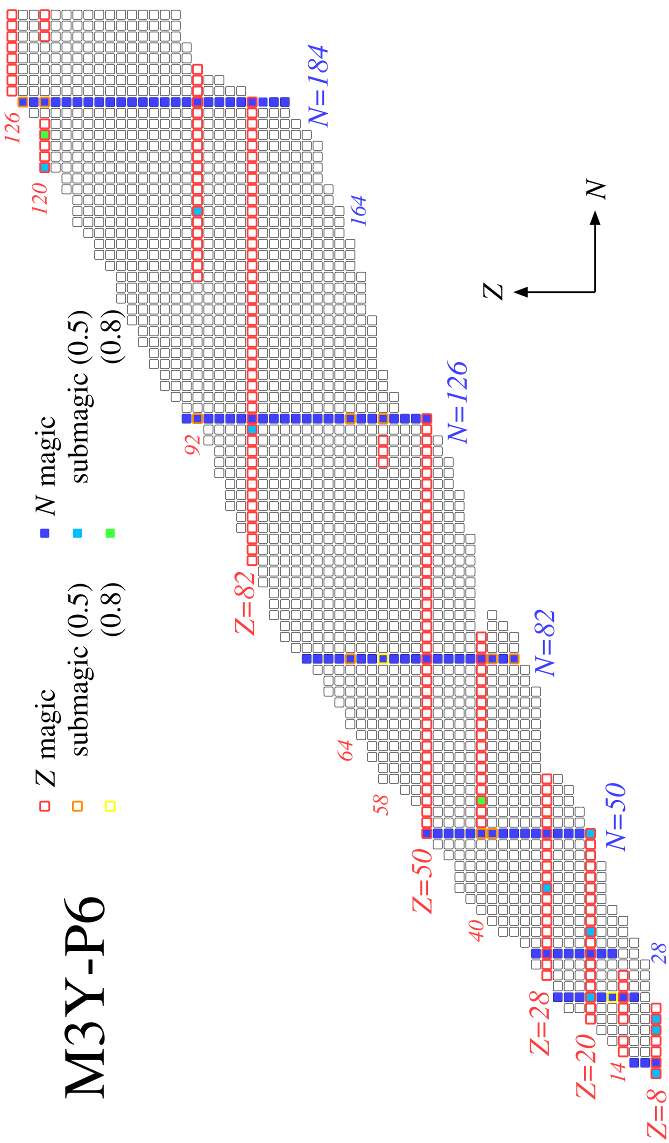

Fig. 2. (Color on-line) Chart showing magic numbers predicted with the M3Y-P6 interaction. Individual boxes correspond to even–even nuclei. Magic (submagic) Zs are represented by the red-colored (orange- or yellow-colored) frame, and magic (submagic) Ns by filling the box with the blue (skyblue or green) color. The $\lambda_{\rm sub}$ values for the submagic numbers (in MeV) are as parenthesized. Quote from Ref. [6].

Magic proton (neutron) numbers may appear at Z (N) which gives certain shell closure in the spherical HF regime. However, this magicity can be broken due to the pair correlation or the deformation, if the shell gap is not sufficiently large. We here take the pair correlation as a measure of the shell gap. Magic Z (N) is assigned if the proton (neutron) pair energy vanishes in the spherical Hartree–Fock–Bogolyubov (HFB) calculations. As submagic numbers are sometimes argued, they are here identified if the energy gain in HFB relative to HF is smaller than a certain value $\lambda_{\rm sub}$. It has been found [6] that magic and submagic numbers obtained from the M3Y-P6 interaction are compatible with most of the available experimental data, as depicted in Fig. 2. For $\lambda_{\rm sub}$, 0.5 and 0.8 MeV are adopted. Although the loss of $N = 20$ magicity at ^{32}Mg [18] and of $Z = 40$ in $N \geq 60$ [19] is not well reproduced in Fig. 2, the axial HF calculation indicates that there is a prolate minimum with close energy to the spherical one at ^{32}Mg [20], and that the absolute minimum is at the prolate in $^{60-66}$Zr [21]. Influence of $\hat{v}_{ij}^{(\rm TN)}$ and $\hat{v}_{\rm OPEP}^{(\rm C)}$ on the magic numbers has been reported in Ref. [6].

4. Isotope shifts — evidence of 3*N* LS interaction

Isotope shifts of the $Z =$ magic nuclei, which are expected to be well described in the spherical MF regime, have provided nuclear structure theories with serious problems. One of them is the kink of the isotope shifts at $N = 126$ in Pb, which has been hard to be reproduced without fictitious s.p. level degeneracy or inversion [22, 23].

Recent χEFT analysis [24] suggests that the strength of the LS channel becomes stronger as the density increases, if the density-dependent $2N$ interaction deduced from the three-nucleon ($3N$) interaction is taken into account. This effect may account for the missing fraction of the ℓs splitting. Instead of enhancing $\hat{v}_{ij}^{(\rm LS)}$ of the M3Y-Paris interaction, in Ref. [10] $\hat{v}_{ij}^{(\rm LS\rho)}$ is added so as not to change the $n0i$ splitting at ^{208}Pb. The new parameter-set, in which all the parameters are identical to those of M3Y-P6 except the LS channels, is named M3Y-P6a.

4.1. Pb isotopes

The χEFT-inspired density-dependent LS interaction may be relevant to the kink problem of the isotope shifts of the Pb nuclei [10].

The isotope shifts of the Pb nuclei are usually defined by adopting ^{208}Pb as a reference, $\Delta\langle r^2\rangle_p(^A{\rm Pb}) = \langle r^2\rangle_p(^A{\rm Pb}) - \langle r^2\rangle_p(^{208}{\rm Pb})$. It has been clarified [22, 25] that the kink at $N = 126$ occurs because of the partial occupation of $n0i_{11/2}$ via the pairing. However, in the studies so far, the kink was reproduced fairly well only by models in which $n1g_{9/2}$ and $n0i_{11/2}$ are almost degenerate or even inverted, although $n1g_{9/2}$ is the lowest orbit above $N = 126$ as confirmed by the energy levels of ^{209}Pb [26]. The channel $\hat{v}_{ij}^{(\mathrm{LS}\rho)}$ tends to extend the s.p. function of the $j = \ell - 1/2$ orbits, *e.g.* that of $n0i_{11/2}$, while tends to shrink those of $j = \ell + 1/2$. Owing to this mechanism, the HFB calculations with M3Y-P6a, in which $\hat{v}_{ij}^{(\mathrm{LS}\rho)}$ is properly combined with the semi-realistic interaction, describe the kink fairly well as shown in Fig. 3, simultaneously giving appropriate s.p. energy difference between $n1g_{9/2}$ and $n0i_{11/2}$ [10].

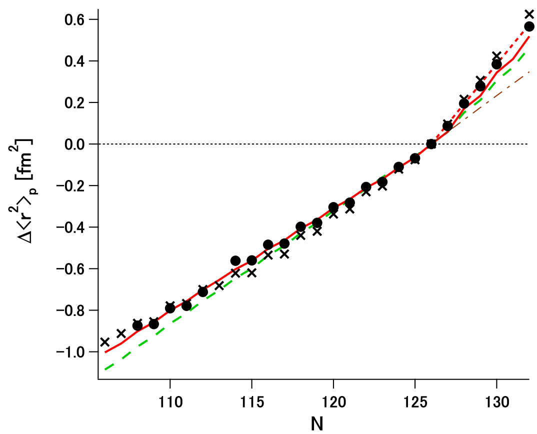

Fig. 3. (Color on-line) Isotope shifts of the Pb nuclei $\Delta\langle r^2\rangle_p(^A\mathrm{Pb})$, obtained from the HFB calculations with M3Y-P6a (solid red line), in comparison to those with M3Y-P6 (dashed green line). Thin brown dot-dashed line in $N \geq 126$ is the HF result in which all the valence neutrons occupy $n1g_{9/2}$. Dotted (red) line shows $\Delta\langle r^2\rangle_p(^A\mathrm{Pb})$ with M3Y-P6a in the hypothetical limit that $n1g_{9/2}$ and $n0i_{11/2}$ were equally occupied. Experimental data are taken from Refs. [27] (circles) and [28] (crosses). Quote from Ref. [10].

4.2. Ca and Sn isotopes

The M3Y-P6a interaction has extensively been applied to the isotope shifts of the Ca and Sn nuclei [29].

As doubly-magic nuclei, both of ^{40}Ca and ^{48}Ca are expected to be well described within the spherical MF calculations. However, the measured isotope shift between them, which is nearly zero, has been hard to be reproduced by self-consistent MF calculations. Remarkably, this problem seems to be solved in the MF calculations with M3Y-P6a, as a result of $\hat{v}_{ij}^{(\mathrm{LS}\rho)}$. See Ref. [29] for the detailed discussion.

The isotope shifts are well reproduced by the spherical HFB calculations with M3Y-P6a in a long chain of the Sn nuclei. In addition, a kink is newly predicted at $N = 82$, by a mechanism similar to the Pb case. Measurement of the isotope shifts above ^{132}Sn is of particular interest, in order to confirm the picture based on the $3N$ LS interaction.

5. Summary

Recent progress via the semi-realistic interaction with respect to the nuclear mean fields is presented. The magic and submagic numbers predicted with the M3Y-P6 interaction are compatible with almost all available experimental data with only a few exceptions from light to heavy stable and unstable nuclei. Although the prediction based on the quenching of the pair correlation gives disagreement in ^{32}Mg and in Zr with $N \gtrsim 60$, this may be lifted if the quadrupole deformation is taken into account. A part of this success is attributed to the realistic tensor force included in the interaction. Effects of the χEFT-inspired density-dependent LS interaction on the isotope shifts of the $Z =$ magic nuclei are clarified. The kink of the Pb nuclei and the vanishingly small shift between ^{40}Ca and ^{48}Ca, both of which have supplied long-standing problems, are well described. Thus, although applications of the semi-realistic interactions have yet been limited, the semi-realistic interaction is suitable for investigating certain aspects of the nuclear mean fields, demonstrating that proper combination of microscopic theories and phenomenology on effective interactions can advance nuclear structure physics.

This work is financially supported as KAKENHI Nos. 24105008 and 25400245.

REFERENCES

[1] K. Andō, H. Bandō, *Prog. Theor. Phys.* **66**, 227 (1981).
[2] O. Sorlin, M.-G. Porquet, *Prog. Part. Nucl. Phys.* **61**, 602 (2008).
[3] H. Nakada, *Phys. Rev. C* **68**, 014316 (2003).
[4] H. Nakada, *Phys. Rev. C* **87**, 014336 (2013).
[5] H. Nakada, *Phys. Rev. C* **81**, 051302(R) (2010).
[6] H. Nakada, K. Sugiura, *Prog. Theor. Exp. Phys.* **2014(3)**, 033D02 (2014).
[7] T. Shizuma *et al.*, *Phys. Rev. C* **78**, 061303(R) (2008).
[8] H. Nakada, T. Inakura, H. Sawai, *Phys. Rev. C* **87**, 034302 (2013).
[9] N. Anantaraman, H. Toki, G.F. Bertsch, *Nucl. Phys. A* **398**, 269 (1983).

[10] H. Nakada, T. Inakura, *Phys. Rev. C* **91**, 021302(R) (2015).

[11] H. Nakada, M. Sato, *Nucl. Phys. A* **699**, 511 (2002) [*Erratum ibid.* **714**, 696 (2003)].

[12] H. Nakada, *Nucl. Phys. A* **764**, 117 (2006) [*Erratum ibid.* **801**, 169 (2008)].

[13] H. Nakada, *Nucl. Phys. A* **808**, 47 (2008).

[14] T. Otsuka *et al.*, *Phys. Rev. Lett.* **95**, 232502 (2005).

[15] P. Doll, G.J. Wagner, K.T. Knöpfle, G. Mairle, *Nucl. Phys. A* **263**, 210 (1976).

[16] C.A. Ogilvie *et al.*, *Nucl. Phys. A* **465**, 445 (1987).

[17] H. Nakada, K. Sugiura, J. Margueron, *Phys. Rev. C* **87**, 067305 (2013).

[18] S. Takeuchi *et al.*, *Phys. Rev. C* **79**, 054319 (2009).

[19] T. Sumikama *et al.*, *Phys. Rev. Lett.* **106**, 202501 (2011).

[20] Y. Suzuki, H. Nakada, S. Miyahara, in preparation.

[21] S. Miyahara, H. Nakada, under progress.

[22] P.-G. Reinhard, H. Flocard, *Nucl. Phys. A* **584**, 467 (1995).

[23] P.M. Goddard, P.D. Stevenson, A. Rios, *Phys. Rev. Lett.* **110**, 032503 (2013).

[24] M. Kohno, *Phys. Rev. C* **86**, 061301(R) (2012) [*Erratum ibid.* **88**, 064005 (2013)].

[25] M.M. Sharma, G. Lalazissis, J. König, P. Ring, *Phys. Rev. Lett.* **74**, 3744 (1995).

[26] R.B. Firestone *et al.*, *Table of Isotopes*, 8^{th} edition, John Wiley & Sons, New York 1996.

[27] P. Aufmuth, K. Heilig, A. Steudel, *At. Data Nucl. Data Tables* **37**, 455 (1987).

[28] I. Angeli, K.P. Marinova, *At. Data Nucl. Data Tables* **99**, 69 (2013).

[29] H. Nakada, *Phys. Rev. C* **92**, 044307 (2015).